Thermodynamic, Thermomechanical, and Structural Properties of a Hydrated Asymmetric Phosphatidylcholine

Tong Zhu and Martin Caffrey

Department of Chemistry, The Ohio State University, Columbus, Ohio 43210 USA

ABSTRACT   1-Behenyl-2-lauryl-sn-glycero-3-phosphocholine (22/12 PC) belongs to a unique group of phospholipids in which the molecule has one acyl chain almost twice as long as the other. The temperature-composition phase diagram for this lipid in the range of 25–65°C, and 0 to 84.3% (w/w) water has been constructed by using the isoplethal method in the heating direction and x-ray diffraction for phase identification and structure characterization. At water contents between 10.3 and 34% (w/w) and at temperatures below 43°C, a single mixed interdigitated lamellar gel phase (L_β^m, ▐══▌) of the type described by Hui et al. (1984. *Biochemistry.* 23:5570–5577) and McIntosh et al. (1984. *Biochemistry.* 23:4038–4044) was found. A second phase consisting of bulk aqueous solution coexists with the L_β^m phase at hydration levels above 34% (w/w) water in the temperature range between 25 and 43°C. Above 43°C, a partially interdigitated lamellar liquid crystalline (L_α^p) phase (▐∿∿▌) is seen in the water concentration range extending from 0 to 84.3% (w/w). The pure L_α^p phase is found below 43% (w/w) water, while coexistence of the L_α^p phase and the bulk aqueous solution is observed above this water concentration which marks the hydration boundary. Interestingly, the latter boundary for both L_β^m and L_α^p phases is nearly vertical in the temperature range studied. Furthermore, the lamellar chain-melting transition temperature appears to be relatively insensitive to hydration in the range 0–85% (w/w) water.

We have confirmed the identity of the L_β^m phase by constructing a 5.7-Å resolution electron density profile on oriented samples by the swelling method. Temperature-induced chain melting effects an increase in lipid bilayer thickness suggesting that the L_α^p phase has chains packed in the partially as opposed to the mixed interdigitated configuration. Unlike the symmetric phosphatidylcholines a ripple ($P_{\beta'}$) phase was not found as an intermediate between the low and high temperature lamellar phases of 22/12 PC.

The specific volume of 22/12 PC is 940 ($\pm$1) µl/g and 946 ($\pm$1) µl/g in the hydrated lamellar gel state at 28 ($\pm$2) and 40 ($\pm$2)°C, respectively, from neutral buoyancy experiments.

Based on measurements of the temperature dependence of the various lattice parameters of the different phases encountered in this study the corresponding lattice thermal expansion coefficients have been measured. These are discussed and their dependence on lipid hydration is reported.

INTRODUCTION

Membrane lipid composition analysis studies have shown that hydrocarbon chain length inequality at the sn-1 and sn-2 positions of the glycerol backbone is a feature common to natural glycerolipids (Small, 1986). It is surprising, therefore, that the bulk of the work reported in the literature to date concerns the more, so-called, symmetric lipids where both chains are of identical or similar chain length and degree, position, and isomeric type of unsaturation. This emphasis most likely reflects ease of synthesis and commercial availability of symmetric lipids. Of late, however, there has been

an increased interest in the asymmetric lipids, the phosphati-dylcholines (PC) in particular. For example, several groups have set about investigating systematically the influence of chain length inequivalence on thermotropic mesomorphism and lipid miscibility (Mattai et al., 1987; Wang et al., 1990; Lin et al., 1990, 1991; Bultmann et al., 1991a; Huang, 1991). The benefits of such a study include establishing the fundamental principles upon which the molecular structure-mesophase behavior relationship is based. This, in turn, will enable us to address the question of why such variety exists in the lipid composition of biomembranes and should provide a reliable basis for the rational design of model and reconstituted membranes. The database of such information is still under development, but its scope and size are growing steadily (Caffrey et al., 1991b).

In any discussion of the asymmetric glycerolipids it is necessary to introduce a measure of chain asymmetry or inequivalence by defining the quantity $\Delta C/CL$ referred to as the normalized chain-length difference (Mason et al., 1981). Here

$$\Delta C = |n1 - n2 + 1.5| \qquad (1)$$

is the effective chain-length difference, and $n1$ and $n2$ are the number of carbons in the chains at the sn-1 and sn-2 positions of the glycerol backbone, respectively. The constant 1.5 is introduced to take account of the effective sn-2 chain length shortening due to a bend in the chain between the β and γ methylene units (Zaccai et al., 1979). CL is the effective length of the longer of the two chains and is defined as

$$CL = \begin{cases} n1 - 1, & \text{if } sn\text{-1 is the longer chain} \\ n2 - 2.5, & \text{if } sn\text{-2 is the longer chain} \end{cases} \qquad (2)$$

A cartoon representation of an asymmetric lipid is shown in Fig. 1 which serves to illustrate the meaning of the various terms just introduced. Thus, for example, 22/12 PC has a $\Delta C/CL$ value of $[(|22 - 12 + 1.5|)/(22 - 1) =]$ 0.548, while that of 1-palmitoyl-2-stearoyl-sn-glycero-3-phosphocholine (16/18 PC) is $[(|16 - 18 + 1.5|)/(18 - 2.5) =]$ 0.032. Accordingly, a $\Delta C/CL$ value of 0.5 indicates that the longer chain is about twice as long as the length mismatch between the two chains. In contrast, a $\Delta C/CL$ value of zero corresponds to a lipid where the methyl terminus of the two chains is in perfect registry.

As part of the study introduced above, the Huang group investigated the effect that chain length inequivalence has on the chain order/disorder transition temperature (T_m) and enthalpy change (ΔH) in PCs with an identical molecular weight (Bultmann et al., 1991a; Huang, 1991; Lin et al., 1991; Wang et al., 1990). This amounts to exchanging methylene groups between the sn-1 and sn-2 chains to alter their relative lengths while at the same time holding molecular weight constant. The following results were obtained. T_m and ΔH decrease linearly as $\Delta C/CL$ increases in the range 0.09–0.40. This suggested that the mixed-chain PCs are packed in the lamellar gel phase in a manner similar to that found in the L_β or $L_{\beta'}$ phase of the symmetric
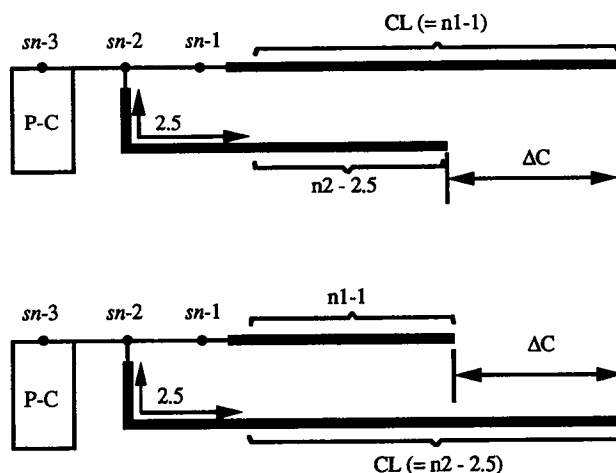
FIGURE 1   Cartoon representation of asymmetric phosphatidylcholines to illustrate the meaning of the terms used to describe normalized chain length difference $\Delta C/CL$. The phosphocholine headgroup is labeled P-C, and the three glycerol backbone carbons are identified appropriately as sn-1, -2, and -3. The number of carbons in the fatty acyl chains at the sn-1 and sn-2 positions are $n1$ and $n2$, respectively. The overall geometry of the molecule is based on the neutron diffraction measurements of Büldt et al. (1978) on DPPC. A more complete definition of ΔC and CL is given in the text.

PCs. The decrease in T_m indicates, however, that lipid-lipid interactions weaken and are progressively perturbed as chain length inequivalence grows. Beyond a $\Delta C/CL$ value of 0.4 and up to 0.67 the dependence on T_m and ΔH on chain asymmetry is bell-shaped with a maximum at $\Delta C/CL$ = 0.57. It is proposed that in this region of relatively large chain inequivalence, the lipid packing geometry within the bilayer changes dramatically with the chains adopting the so-called mixed interdigitated arrangement (L_β^m (Hui et al., 1984; McIntosh et al., 1984)). The characteristics of the L_β^m phase will be discussed further below. What is interesting about this latter group of lipids is that the longer of the two acyl chains has an effective chain length in the gel phase which is approximately double that of the chain length inequivalence. In this study, we focus on one of these lipid species, viz., 22/12 PC, which has a $\Delta C/CL$ value of 0.548, right in the middle of the $\Delta C/CL$ range where the L_β^m phase is proposed to exist. It has two saturated fatty acyl chains which are 22 (behenyl) and 12 (lauryl) carbon atoms long in ester linkage at the sn-1 and sn-2 positions, respectively, of the glycerol backbone. 22/12 PC is referred to as a mixed chain lipid where mixed indicates that the two acyl chains are different. To date, a limited amount of calorimetric data but no structure or miscibility information is available on this "pivotal" lipid species. We wished to improve on this deficit by performing a study incorporating the following objectives: to establish mesophase identity and to characterize structurally, thermodynamically, and thermomechanically the various mesophases that exist in the temperature-composition phase diagram of the 22/12 PC-water system in the temperature range of 25 to 65°C and in the composition range from 0 to 85% (w/w) water.

EXPERIMENTAL PROCEDURES

Materials

The 22/12 PC lipid was kindly provided by Professor Ching-hsien Huang (Department of Biochemistry, University of Virginia, Charlottesville, VA) and was used without further purification. The lipid had a purity of between 98 and 99% as judged by thin-layer chromatography on silica gel K5F plates (Alltech Assoc. Inc., Deerfield, IL) with three solvent systems (chloroform/methanol/water, 65:25:4 by volume; chloroform/methanol/29.8% (w/w) ammonium hydroxide, 65:25:5 by volume; chloroform/methanol/acetone/acetic acid/water, 10:2:4:2:1 by volume). For purposes of constructing the temperature-composition phase diagram and for phase mensuration we assume that the lipid "as received" is anhydrous. It is likely that the lipid has at least one or two associated water molecules per lipid molecule under these conditions. Throughout the text we use the term "dry" to refer to the "as received" lipid to which bulk water has not been added. Water was obtained from a Milli-Q water purification system (Millipore Corp., Bedford, MA). D_2O (D, 99.996%) was obtained from Cambridge Isotope Laboratories (Woburn, MA). Analytical reagent grade NaBr and $Pb(NO_3)_2$ were from Mallinckrodt Inc. (Paris, KY). KCl was from Jennelle Chemical Co. (Cincinnati, OH). NaCl was from Morton Salt (Rittman, OH).

X-ray diffraction of powder samples

Sample preparation

The powder samples at various water concentrations were prepared in 0.7-mm diameter (10-μm wall thickness) quartz capillaries (Charles Supper Co., Natick, MA). The lipid was dropped into a capillary of known weight through a small plastic funnel made from a 0.5–10-μl Ultra Micro Tip (Eppendorf, Brinkmann Instruments, Inc., Westbury, NY). After the loaded capillary was weighed on an electronic micro balance (Micro M3P; Sartørius Co., Bohemia, NY), a defined volume of Milli-Q water was delivered to the top of the capillary and spun down into contact with the lipid by using a bench-top centrifuge (model 428; International Equipment Co., Baxter Healthcare Co, IL). The capillary was reweighed, sealed using a butane-oxygen micro-flame torch (Microflame, Inc., Minnetonka, MN), and further sealed with extra fast setting epoxy (04001; Hardman Inc., Belleville, NJ). To obtain a homogeneous sample, the hermetically sealed capillary was heated to between 65 and 70°C in a Multi-Block Heater (H2025–1A; Lab-Line Instruments, Melrose Park, IL) for 5 min and then cooled to room temperature (approximately 25°C). This heating and cooling process was repeated four times.

Two dry samples were also prepared. The lipid was packed into the capillary and sealed in the same way as described above with the exception that no water was added. One of the dry samples experienced the heating and cooling cycles as above. The other was not preheated.

All samples were stored at 2–4°C until 2 h before the x-ray diffraction measurements were made.

X-ray source

The diffraction experiments on powder samples were carried out with wiggler-enhanced, monochromatic synchrotron radiation on the A1 and F1 lines at the Cornell High Energy Synchrotron Source (CHESS). In the A1 station, time-resolved x-ray diffraction measurements were made using focused x-rays as previously described (Caffrey 1985, 1987). The machine was operated at 5.26 GeV, with an 80-mA electron beam current in the seven-bunch mode, and with the six-pole wiggler at half-power. The F1 station was operated at a 90-mA total of positron beam current with wiggler radiation from a 25-pole, 1.2-Tesla permanent magnet insertion device. Detailed information on the F1 line has been described previously (Chung and Caffrey, 1992). The x-ray wavelength used in the A1 (1.561 Å) and F1 (0.912 Å) stations was determined using a lead nitrate standard and a carefully measured sample-to-film distance. The incident x-ray beams were defined using a 0.3-mm diameter collimator (Charles Supper Co., Inc., Natick, MA). The x-ray flux through the collimator was of order 10^{10} photons/s in both A1 and F1 stations measured using an ion chamber.

Data were also collected on the X12B line at the Brookhaven National Synchrotron Light Source (NSLS). X-ray wavelength (0.912 Å) was determined by using a cholesterol myristate standard and a carefully measured sample-to-film distance. The optical arrangement at the X12B station enabled focusing of the beam to a point approximately 0.5-mm wide and 2-mm high at the detector. The optical configuration at X12B has been described previously (Chung and Caffrey, 1992).

Diffraction measurements

The experimental arrangement for making powder x-ray diffraction measurements has been described previously (Mencke and Caffrey, 1991). In addition, a home-built sample holder was used, the central part of which consists of a brass or beryllium cell in thermal contact with two thermoelectric (Peltier) devices via a copper block. A small window in the brass cell is covered with Metalon aluminized film (Type C(15), 0.0005-inch thick, Alexander Vacuum Research, Inc., Greenfield, MA) to provide a more uniform thermal environment for the samples. The cell assembly is housed in an aluminum box fitted with two thin beryllium windows. The entire sample holder is attached to two motorized and remotely controlled translation stages that allow positioning in both the vertical and horizontal directions. These motors and the temperature of the cell are all under computer (Macintosh IIfx) control using LabVIEW (National Instruments Co., Austin, TX) software.

A streak camera was used to record live-time x-ray diffraction patterns continuously as a function of temperature. This camera has an adjustable vertical slit through which the diffracted x-rays pass before being recorded on x-ray sensitive film (DEF-5; Kodak, Rochester, NY) and/or image plates (Kodak storage phosphor; Kodak). The latter are translated at a constant speed behind the slit controlled by LabVIEW software as above. Because a finite slit width is used, data collected with the streak camera have time and temperature resolution compromised somewhat in the present application. For example, with a 2.2-mm wide slit and a film translation speed of 6 mm/min, each spatial element on the film or plate is exposed for ≤ [2.2 mm/(6 mm/min =] 0.4 min (24 s). With a temperature scan rate of 2°C/min, the corresponding temperature range that each spatial element samples is ≤[2°C/min × 0.4 min =] 0.8°C.

The isoplethal temperature-composition phase diagram was constructed in the designated temperature and composition range as follows. Each sample of fixed hydration was heated at a rate of 2°C/min from 25 to 65°C, incubated at 65°C for 5 min, and then cooled to 25°C at the rate of 2°C/min. The x-ray sensitive film (5 × 7 inch) moving behind a 2.2- (CHESS) or 2.75-mm (NSLS) vertical slit at the speed of 4.2 or 6 mm/min (depending upon the strength of the x-ray beam), was used to record both low- and wide-angle diffraction patterns simultaneously. Continuous translation of the capillary sample back and forth in and perpendicular to the x-ray beam over a 3–5-mm range at a rate of 5 mm/s during the entire exposure limited the degree of x-ray damage to the sample. At no point in the course of these measurements was any one part of the sample exposed to the beam for longer than 4 min. Experiments to test for radiation damage were performed following a previous description protocol (Caffrey, 1984; Cheng et al., 1993). In one test on the X12B line at NSLS, the fully hydrated sample was exposed continuously to the x-ray beam for 30 min at 40°C, and a separate diffraction pattern was recorded every 2 min. In another test on the A1 line at CHESS, the diffraction patterns were recorded continuously as a function of time at room temperature (ca. 24°C) for 1 h using the streak camera. No damage was observed during the first 10 min of exposure in both tests. At longer exposure times, the diffraction pattern begins to fade.

To complement the streak film data high resolution two-dimensional diffraction patterns were recorded periodically on stationary x-ray-sensitive film.

X-ray diffraction of oriented samples

Sample preparation

To construct the electron density profiles of the lamellar gel phase, oriented samples were prepared as follows. Forty μl of ~0.2 mg of lipid/μl chlo-

roform solution was placed on a 0.8–1.0-mm-thick micro glass slide (~2.5 cm^2 in area; Objekttrager, Porte-objects, Switzerland) in 8-μl increments. After each deposition, the sample was placed in a closed glass chamber (3-inch diameter, 1.5 inches high) containing a separate reservoir of chloroform to allow the solvent in the sample to evaporate slowly (in ~5 min) thereby facilitating the formation of highly oriented lamellae. The sample was stored subsequently in an empty glass dish covered loosely with filter paper to allow air exchange at room temperature for 24 h to deplete further the solvent content of the sample. The sample was transferred to a humidity-controlled diffraction cell (~1.5-inch diameter) containing two shallow wells filled with a saturated salt solution which serves to fix the relative humidity (RH) within the cell. The cell was sealed with a screw cap and vacuum grease (Dow Corning Co., Midland, MI). A Kapton (K-104; XTO Inc., Johnson City, NY) window through which x-rays can pass is provided in the side of the cell. The following salt solutions were used to provide atmospheres of increasing RH: NaBr, 57.0% RH; NaCl, 75.5% RH and KCl, 84.6% RH (O'Brien, 1948). Oriented samples were incubated at each RH for at least 24 h at 28 ($\pm$2)°C before the diffraction measurements were made at 28 ($\pm$2)°C.

Diffraction measurements

A Rigaku, Geigerflex camera with D/MAX-B system software (Danvers, MA) was used to collect θ–2θ diffraction scans on oriented samples. The x-ray tube was operated at 40 KV and 30 mA. The 1/6° divergence slit was used to fix the horizontal divergence angle of the x-ray beam irradiating the sample. A receiving slit with an aperture width of 0.15 mm and the 1/6° scattering slit were placed on the downstream side of the sample to reduce unwanted scattered x-rays from striking the counter. A 0.021-mm-thick nickel filter (0.019 g/cm^2) was placed in front of the receiving slit to allow the CuK α radiation at 1.541 Å to enter the counter.

To check that the hydrated lipid bilayers were well oriented on the glass slide, a quick diffraction measurement was made in the 1° < 2θ < 25° range. The absence of sharp reflections from the acyl chains in the region between 20 and 25° indicated that the sample was indeed highly oriented. Subsequent θ–2θ scans were recorded from 1 to 21° in steps of 0.01° at a rate of 0.03°/min at 28 ($\pm$2)°C. Each complete diffraction pattern was collected in about 11 h.

Electron density profile determination

To decipher hydrocarbon chain-packing conformation in the lamellar gel phase, the diffracted intensity distribution in the θ–2θ scan was analyzed to yield one-dimensional electron density profiles as described previously (Caffrey et al., 1991b) with the following modification. The integrated intensity of each reflection was calculated by using the *Integrate-Area* function under *Macro menu* of KaleidaGraph software (Version 2.1; Synergy Software, Reading, PA).

Specific volume

A neutral buoyancy technique (Caffrey et al., 1991a) was used to measure the specific volume of the lipid in the lamellar gel phase. A series of H_2O/D_2O solutions of various densities were prepared in 2-mm diameter quartz capillaries (Charles Supper Company, Natick, MA). A 50-μl syringe (Hamilton Co., Reno, NV) was used to deliver the H_2O/D_2O solution into the capillary to which was added the dry lipid powders. The capillary was then sealed with the micro flame torch followed by epoxy glue as described above, centrifuged in a bench-top centrifuge, and kept in a Multi-Block Heater (H2025–1A; Lab-Line Instruments, Melrose Park, IL) at 28 ($\pm$2)°C and 40 ($\pm$2)°C for 5 days before making the final observations. The density of H_2O and D_2O is 0.996 and 1.104 g/ml at 28°C and 0.992 and 1.100 g/ml at 40°C (CRC Handbook). The specific volume of the lipid, v_1, was determined from the H_2O/D_2O mixture giving neutral buoyancy with an estimated accuracy of 1 μl/g.

RESULTS

Specific volume

The specific volume of fully hydrated 22/12 PC multilamellar vesicles was measured by the neutral buoyancy method at 28 ($\pm$2) and 40 ($\pm$2)°C as described under Experimental Procedures. The corresponding values are 940 ($\pm$1) and 946 ($\pm$1) μl/g for the lipid in the lamellar gel phase which correspond to a molecular volume of 1188 and 1196 Å^3 given a molecular weight of 761 g/mole.

Hydrated lipid

As a structural complement to previously performed calorimetry measurements (Lin et al., 1990), low- and wide-angle x-ray diffraction measurements were performed on hydrated 22/12 PC. Both static and time-resolved streak film data were collected. The static two-dimensional diffraction patterns (data not shown) were recorded at selected temperatures in the range of interest as a check on the veracity of the streak film data, since the former offer superior sensitivity and resolution. In every instance, the static and streak film data were in agreement in regard to both intensity and d-spacing of the various reflections in the pattern. A selection of streak film data recorded in the heating and cooling directions in the 25 to 65°C range through the chain order/disorder transition, T_m, is shown in Fig. 2. The corresponding phase designation is included in Fig. 2 A.

In the low-angle region below T_m, four lines are apparent which index on a one-dimensional lamellar lattice with d_{001} = 52.2 Å at 28°C and 18.6% (w/w) water concentration (Fig. 2 A). The reflections are uniformly sharp from 25°C up to T_m and show little sensitivity to temperature in this range. The intensity of each reflection as a function of order (l) is as follows: strong ($l = 1$), medium ($l = 2$), medium ($l = 3$), weak ($l = 4$). The wide-angle region of the diffraction pattern is dominated by a single, strong, sharp, and symmetric reflection with an obvious d-spacing dependence on temperature (negative thermal expansion coefficient). At 28°C, the d-spacing value of this reflection is 4.13 Å. For now, this phase is designated as a lamellar gel (L_β) phase with chains oriented perpendicular to the plane of the lipid bilayer.

A dramatic change in phase is observed in the streak film at 43°C when chain "melting" occurs. This is evidenced by a loss of the sharp wide-angle reflection which is replaced by a broad, diffuse scattering band centered at ~4.5 Å (not apparent in the photograph shown in Fig. 2 A, but obvious in the original streak film and on the corresponding static two-dimensional patterns). Simultaneously, a new set of lamellar reflections emerge in the low-angle region which are uniformly sharp and not particularly temperature sensitive in the range of 43 to 65°C. The corresponding lamellar repeat for this lamellar liquid crystal (L_α) phase is d_{001} = 53.0 Å at 60°C. A slight increase in the diffuse scattering background in the low-angle region accompanies the emergence of the L_α phase.
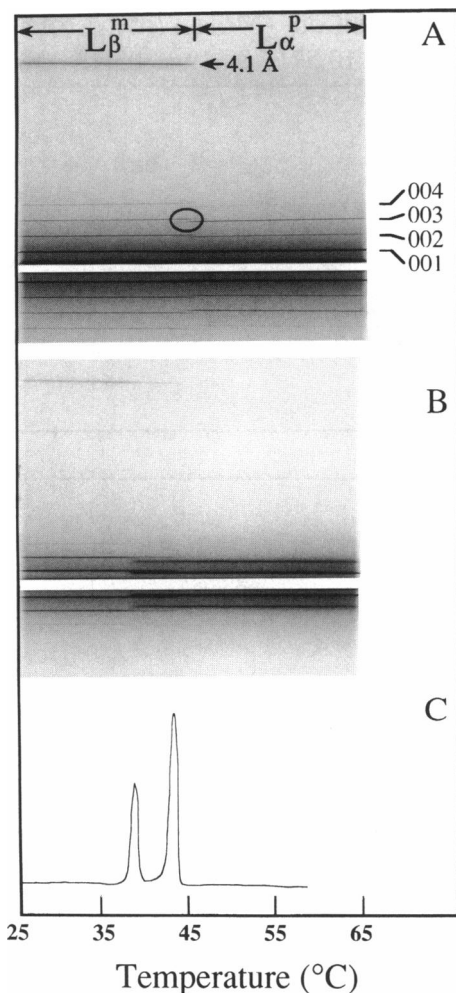
FIGURE 2   Low- and wide-angle time-resolved x-ray diffraction patterns of hydrated 22/12 PC powder samples recorded on a translating streak film during heating (A) and cooling (B) at 2°C/min in the 25–65°C range. The film was translated at a rate of 6 mm/min behind a 2.2-mm-wide vertical slit. Samples were hydrated at 18.6% (w/w) water (A) and 58% (w/w) water (B). Measurements were performed on the A1 station at CHESS ($\lambda = 1.561$ Å) with a sample-to-film distance of 18.7 cm and a 0.3-mm diameter collimator. For scale, the distance between the lamellar reflections in the L_β phase on the original x-ray film is approximately 8 mm. (C) The first cooling DSC thermogram of an aqueous dispersion of 22/12 PC recorded at 5–15°C/h on 60 to 25°C (adapted from Fig. 7 of Lin et al. (1990)).

The L_β/L_α phase transition as observed in the streak film data shown in Fig. 2 A is quite sharp. Phase coexistence is apparent in a narrow temperature range as the simultaneous presence of the low-angle reflections from the L_β and L_α phases with distinctly different lattice parameters. As temperature increases from left to right in the figure the relative intensity of the L_β phase decreases while that of the L_α phase increases. There is no evidence for an intermediate in the transition region to within the sensitivity limits of this detection system. This is in marked contrast to the symmetric PCs where the so-called ripple or $P_{\beta'}$ phase exists as an intermediate phase between the lamellar gel and L_α phases.

Upon cooling the fully hydrated samples from the L_α phase, we find by analogy with the calorimetry data (Lin et

al., 1990) that the heating transition is not simply reversed upon lowering temperature (Fig. 2 B). The first marked change in the diffraction pattern occurs at 42°C where a sharp wide-angle line at 4.13 Å appears accompanied by a set of three low-angle lines which index on a lamellar lattice with $d_{001} = 59.4$ Å. Continued cooling at a rate of 2°C/min shows *phase coexistence over the extended temperature range of 5°C*. At 37°C, the last vestiges of the high temperature L_α phase disappear and only the L_β phase, characteristic of the original low temperature phase observed before heating began, remains. What is unusual about the cooling behavior of this fully hydrated lipid is that the relative amounts of the coexisting L_β and L_α phases do not change dramatically in the temperature range of coexistence. Clearly, the transition involves an L_α-to-L_β conversion with the onset and disappearance of coexistence corresponding in temperature to the two exothermic peaks at 42.7 and 38.6°C seen in the corresponding cooling calorimetry traces (Fig. 2 C). The structural origin of the two exothermic events has not been elucidated based on the current x-ray diffraction measurements. Parenthetically, we note that this unusual cooling behavior was observed with fully hydrated lipid only. Simple heating-cooling reversibility prevailed with samples prepared at less than full hydration.

A series of isoplethal measurements in the heating direction has been carried out on 22/12 PC over a range of hydration levels extending to 84.3% (w/w) water. From 10.3 to 84.3% (w/w) water, the only features of the diffraction pattern to change were the lamellar lattice dimensions and the relative intensities of the low-angle reflections for the L_β phase up to 34% (w/w) water and for the L_α phase up to 43% (w/w) water. These data are shown in Fig. 3 where the lamellar repeat for both the L_β and the L_α phases is plotted as a function of water content. At 28°C, the size of the L_β lamellar repeat increases linearly with hydration level from 47.2 Å at 10.3% (w/w) up to a limiting value of ~59 Å at 34% (w/w) water. Thus, 34% (w/w) water marks the maximum water holding capacity of this phase at 28°C. Beyond this limit, additional water forms a separate aqueous bulk phase and does not serve to swell the lipid further.

At 60°C in the L_α phase, the hydration dependence of the lamellar repeat is sigmoidal. Swelling continues up to the hydration limit of 43% (w/w) water where the lamellar repeat stabilizes at 71 Å. An analysis of the streak film data over the full range of hydration shows that the hydration limit is essentially temperature-independent for both the L_β and L_α phases in the temperature range studied. A select set of such data is included in Fig. 4. Thus, in the corresponding temperature-composition phase diagram for the 22/12 PC-water system (vide infra) the boundary separating the single (L_β or L_α) and two phase (L_β or L_α plus bulk aqueous phase) regions is essentially vertical.

Isoplethal measurements were also performed with 22/12 PC in combination with low levels of water corresponding to 4.2 and 6.6% (w/w) water. The latter showed a single low-angle reflection with a d-spacing of 45.8 Å and a single wide-angle reflection at ~4.1 Å at 28°C. The wide-angle
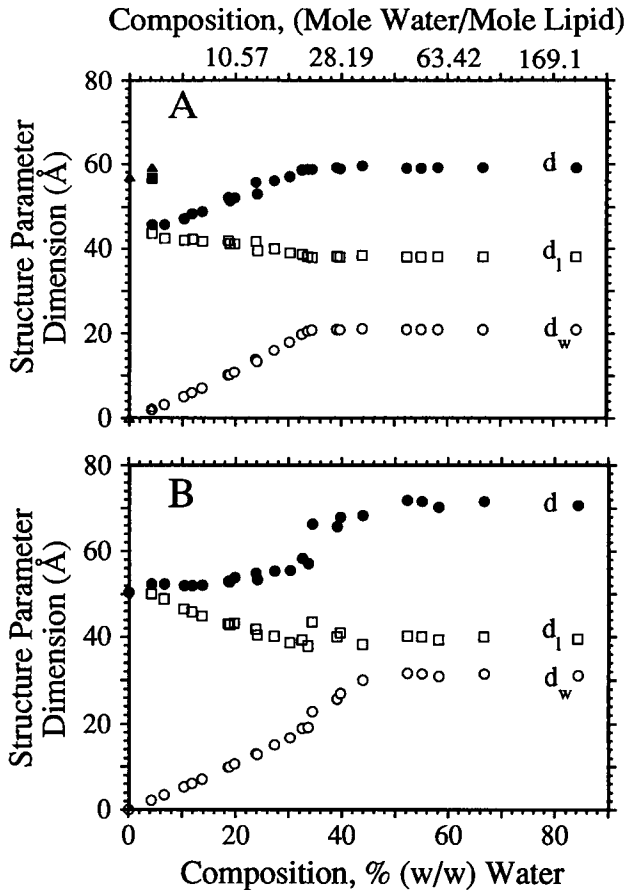
FIGURE 3 Structure parameter dimensions of 22/12 PC as a function of water content expressed in units of % (w/w) water and water-to-lipid mole ratio at 28°C (A) and 60°C (B). (●) Lamellar periodicity, d; (□) lipid bilayer thickness, d_1; (○) water layer thickness, d_w. In A: (▲) lattice repeat distance, (■) lipid bilayer thickness, d_1, and (△) water layer thickness, d_w, were obtained by assuming that the lattice is lamellar.

FIGURE 4 Lamellar periodicity of the L_β^m phase (A) and the L_α phase (B) of 22/12 PC at the following temperatures. In A: (○) 28°C; (●) 35°C; (⊞) 40°C. In B: (◎) 46°C; (⊡) 50°C; (■) 60°C.

behavior suggests β-type chain packing. However, because of there being only a single low-angle reflection the corresponding lattice type and symmetry of the sample cannot be determined unambiguously. Interestingly, the 4.2% (w/w) water sample had an identical wide-angle diffraction pattern to that observed with the 6.6% (w/w) water sample. However, in this case the low-angle region contained just two reflections, one at 45.8 Å and one at 59.2 Å at 28°C. As will be shown below, it is likely that at 4.2% (w/w) water and 28°C the sample consists of coexisting phases—one of which is observed in isolation in the preheated dry sample and the other in isolation at 6.6% (w/w) water. Isoplethal heating and cooling measurements in the 25 to 60°C range show that the transition is reversible at these two hydration levels.

Dry lipid

The diffraction pattern of dry 22/12 PC that had not been heated previously was recorded at 28°C and is shown in Fig. 5. The pattern consists of a series of low-angle reflections which index on a lamellar lattice with d_{001} = 60.3 Å. The

wide-angle is dominated by multiple sharp and broad reflections extending out to 2.79 Å suggesting a crystalline packing of the acyl chains. This phase is identified as being of the lamellar crystalline (L_c) type. Isoplethal measurements made in the 25 to 65°C range shows an L_c-to-L_α phase transition in the range at 40 to 43°C. In the L_α phase at 60°C the lamellar repeat spacing is 50.4 Å. The corresponding wide-angle scattering peak is centered at ~4.5 Å.

In contrast to the non-preheated sample, lipid that had been subjected to the standard heating/cooling cycle indicated under Experimental Procedures produced a relatively simple diffraction pattern at 28°C. The low-angle region indicates lamellar long range order with d_{001} = 56.9 Å, while the wide-angle region of the pattern shows a sharp reflection at 4.21 Å with a relatively weak broad, wide-angle shoulder at 4.19 Å (data not shown) suggesting a tilted acyl chain arrangement. This phase is identified as being of the $L_{\beta'}$ type. A temperature ramping measurement of the pre-heated 22/12 PC in the 25 to 65°C range shows an $L_{\beta'}$-to-L_α phase transition taking place between 41 and 44.1°C. The lamellar repeat spacing of the L_α phase at 60°C is 50.4 Å as was observed for the non-preheated sample. By comparison with the data presented above under Hydrated Lipid, it appears as though elements of the $L_{\beta'}$ phase persist up to a hydration

FIGURE 5   The diffraction pattern recorded at 28°C of non-preheated dry 22/12 PC. Experimental conditions: sample-to-film distance, 20.0 cm; wavelength, 0.92 Å (13.6 KeV); collimator diameter, 0.3 mm; incident flux, 10^{10} photons/s; positron current, 76 mA; machine energy, 5.3 GeV; exposure time, 20 s. The d-spacing values of the various reflections or scattering peaks in this photograph are as follows: 50.6, 25.5, 17.0, 10.2, 10.7, 9.54, 9.13, 7.83, 6.19, 5.86, 5.66, 5.51, 4.55, 4.44, 4.32, 4.22, 4.00, 3.90, 3.85, 3.64, 3.50, 3.40, 3.10, and 2.79 Å.

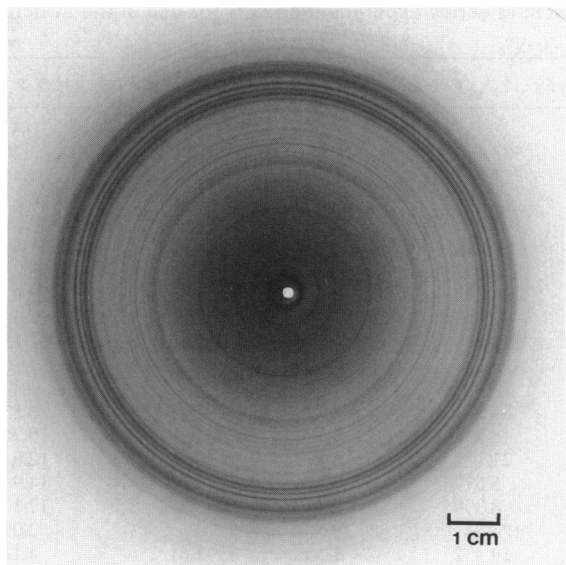level of 4.2% (w/w) water at 28°C. It transforms to the L_β phase at and above 6.6% (w/w) water.

Oriented samples

A θ–2θ scan of the diffracted intensity from an oriented preparation of 22/12 PC at 57.0% RH and 28 ($\pm$2)°C is shown in Fig. 6. The sample was well aligned and revealed a total
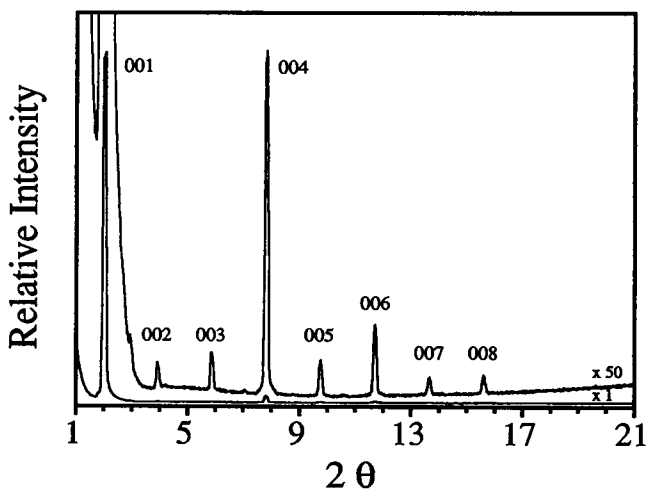

FIGURE 6 θ–2θ diffracted intensity scan of oriented 22/12 PC in the L_β^m phase at 57.0% RH and 28 ($\pm$2)°C. The scan was recorded as described under Experimental Procedures. The lamellar repeat order number is indicated above or next to each peak. The lamellar repeat spacing is 45.4 Å. The upper plot represents a 50-fold vertical scale expansion of the lower plot.

of eight lamellar reflections with d_{001} = 45.4 Å. Upon increasing the RH in a stepwise manner a swelling series was generated. At 75.5 and 84.6% RH, the lamellar repeat spacing had increased to 46.9 and 47.8 Å, respectively. The corresponding number of lamellar reflections was eight and six. Table 1 summarizes the diffraction data from the oriented samples in this swelling series experiment. The normalized structure factor amplitudes ($|Fn(00l)|$) for the swelling series are shown as a function of the reciprocal lattice coordinate s [=$(2/\lambda)\sin\theta$] in Fig. 7. The data collected in the 57.0 to 84.6% RH range fell on a smooth curve indicating that the unit cell, and, thus, the structure of the bilayer, did not change significantly upon hydration. The corresponding electron density profiles obtained from these swelling series data are presented in Fig. 8 for the three hydration levels studied. These profiles suggest that in the L_β phase lipid has acyl chains that interdigitate as will be expanded upon under the Discussion.

DISCUSSION

Membrane mensuration

In what follows, the structure parameters derived from x-ray diffraction measurements are combined with composition and specific volume data to reveal the arrangement of lipid and water in the different lamellar phases observed in this study. An important quantity obtained from the hydration data shown in Fig. 3, where d_{001} (hereafter referred to simply as d) is plotted against water content, is the hydration limit of the phase under investigation. For the low temperature gel phase, this hydration limit occurs at 34% (w/w) water. The corresponding value for the L_α phase is 43% (w/w) water. In both cases, the hydration limit is quite insensitive to temperature in the range studied (Fig. 4). Thus, regardless of the overall water content of the sample, once the hydration limit is exceeded the composition of the phase is that of the hydration limit. Below the limiting hydration level, the water content of the phase is that of the sample overall.

Mesophase mensuration was carried out following standard procedures (Small, 1967; Luzzati, 1968). Thus, lipid bilayer thickness (d_l) is calculated from the experimentally determined lamellar repeat spacing (d), the known lipid and water concentration of the phase (C_l, C_w) and the specific volume of lipid and water (v_l, v_w) as follows:

$$d_l = \left[\frac{C_l v_l}{C_l v_l + C_w v_w}\right] d. \qquad (3)$$

Below the hydration limit

$$C_l = \frac{W_l}{W_l + W_w} \qquad (4)$$

and

$$C_w = 1 - C_l \qquad (5)$$

where W_l and W_w refer to the weight of lipid and water, respectively. Above the hydration limit, the values of C_l and

TABLE 1   Stepwise analysis of θ–2θ data collected on 22/12 PC in a swelling series experiment at 28°C for use in the structure amplitude plot shown in Fig. 7.

RH	00l	2θ	d	d_{ave}	I	$I \times l$	$\lvert F \rvert = \lvert \sqrt{I \times l}\rvert$	$\lvert F \rvert_N$	$\lvert F \rvert_N(d/d_{min})^*$	$(1/d) \times 100$
%		deg	Å	Å						1/Å
57.0	1	1.96	45.0		14682 × 10	14682 × 10	383.17	10.0	10.0	2.20
	2	3.90	45.3		158.18	316.36	17.787	0.464	0.464	4.41
	3	5.84	45.4		237.38	712.14	26.686	0.694	0.694	6.61
	4	7.82	45.2		2517.3	10069	100.35	2.62	2.62	8.81
	5	9.76	45.3		233.83	1169.2	34.193	0.892	0.892	11.0
	6	11.7	45.4		511.19	3067.1	55.382	1.45	1.45	13.2
	7	13.7	45.4		113.90	797.30	28.237	0.737	0.737	15.4
	8	15.6	45.4	45.4	107.75	861.96	29.359	0.766	0.766	17.6
75.5	1	1.95	45.3		58649	58649	242.18	10.0	10.3	2.13
	2	3.81	46.4		116.17	232.34	15.243	0.629	0.650	4.26
	3	5.66	46.8		503.59	1510.8	38.869	1.61	1.66	6.40
	4	7.53	46.9		1084.8	4339.0	65.871	2.72	2.81	8.53
	5	9.40	47.0		68.240	341.20	18.472	0.763	0.788	10.7
	6	11.3	47.1		74.780	448.68	21.182	0.875	0.904	12.8
	7	13.1	47.1		6.3700	44.590	6.6776	0.276	0.285	14.9
	8	15.0	47.2	46.9	8.8000	70.400	8.3905	0.347	0.354	17.1
84.6	1	1.93	45.9		16062	16062	126.74	10.0	10.5	2.09
	2	3.74	47.2		188.80	377.60	19.432	1.53	1.61	4.18
	3	5.56	47.7		368.64	1105.9	33.256	2.62	2.76	6.28
	4	7.37	48.0		544.00	2176.0	46.650	3.68	3.87	8.37
	5	9.19	48.1		19.520	97.600	9.8793	0.780	0.821	10.5
	6	11.0	48.2	47.8	24.255	145.54	12.064	0.952	1.00	12.6

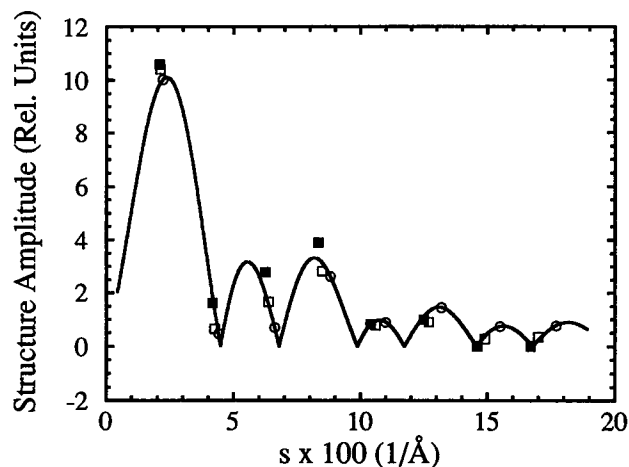* d_{min} is the smallest lamellar repeat d-spacing in the swelling series (d_{min} = 45.4 Å).

FIGURE 7   Modulus of the normalized structure factor amplitude versus reciprocal spacing for 22/12 PC in the L_β^m phase at 28 (±2)°C and 57.0% RH (○), 75.5% RH (□) and 84.6% RH (■). The solid curve was calculated using Shannon's sampling theorem at 57.0% RH as described in the text. The phases assigned to each diffraction order beginning with 001 and ending with 008 are − − + − + − + −.

C_w that correspond to limiting hydration are used in Eqs. 4 and 5. The water layer thickness of the lamellar phase is given by:

$$d_w = d - d_l \tag{6}$$

and the average interfacial surface area per lipid molecule by:

$$S = \frac{2M_l v_l}{d_l N} \tag{7}$$

where M_l is lipid molecular weight and N is Avogadro's num-

ber. Finally, the cross-sectional area per acyl chain assuming hexagonal chain packing in the gel phase is calculated as

$$\Sigma = \frac{2d_c^2}{3^{1/2}} \tag{8}$$

where d_c is the experimentally measured chain-packing repeat spacing (the d-spacing of the 10 wide-angle reflection) at 4.13 Å for the L_β phase and 4.21 Å for the $L_{\beta'}$ phase at 28°C. The quantity S/Σ is a measure of the average number of acyl chains in the bilayer interior that are associated with each lipid headgroup. A complete listing of the d, d_l, d_w, S, Σ, and S/Σ values for the lamellar gel and lamellar liquid crystal phases at 28 and 60°C, respectively, as a function of hydration level is presented in Table 2. Since the acyl chains in the L_α phase do not occupy a regular lattice an estimate of S and Σ is not appropriate for this phase.

The data in Table 2 and in Fig. 3 show that as water content increases up to the hydration limit in both L_β and L_α phases so too do d and d_w. In contrast, d_l decreases slightly but significantly in response to hydration. This type of behavior is common to a host of lipid systems (McIntosh et al., 1984; Shah et al., 1990; Klose et al., 1988; Klose et al., 1992).

A particularly interesting result is obtained when we compare the d_l values of the L_β and L_α phases under conditions of full hydration. The corresponding values are 38.2 and 40.6 Å, respectively. These data rule out a simple chain order-to-disorder transition within the bilayer which would effect a reduction rather than an increase in d_l. Thus, the transition must involve, in addition to chain melting, a structural rearrangement of the lipid molecules relative to one another in the bilayer. This important issue will be elaborated on further when chain packing in the low temperature phase has been discussed.
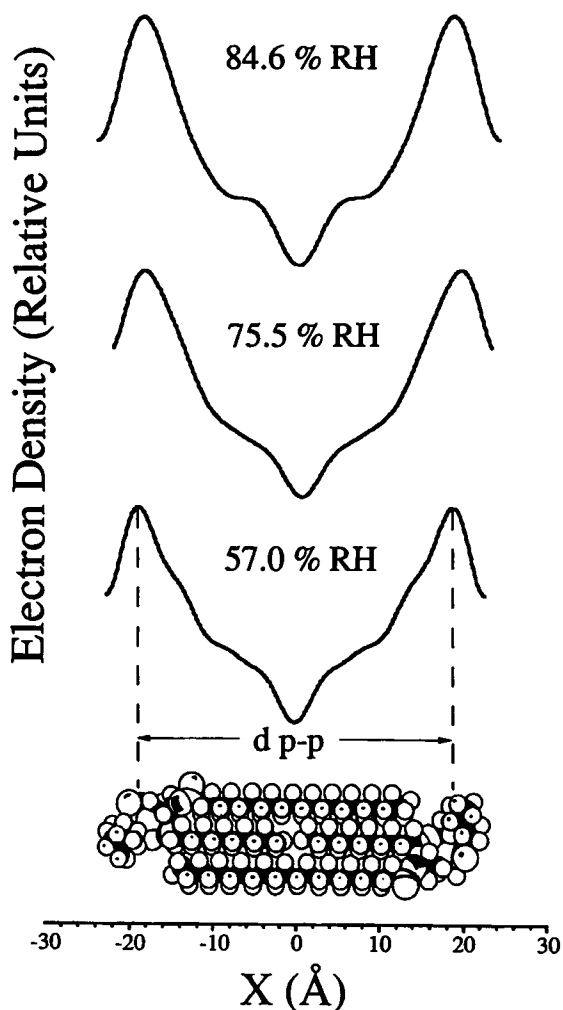
FIGURE 8   One-dimensional electron density profiles of 22/12 PC at 28 (±2)°C and 57.0, 75.5, and 84.6% RH. At 57.0% RH, the lamellar repeat distance is 45.4 Å, the distance between the peaks of highest electron density (dp-p) is 38 Å, and the resolution of the profile is 5.7 Å. The corresponding values for the profile at 84.6% RH are 47.8, 37, and 8.0 Å. The CPK model of 22/12 PC in the L_β^m phase is included at the bottom of the figure for reference.

Electron density profile

As noted above, the structure of the unit cell for the lamellar gel phase of hydrated 22/12 PC does not change significantly upon hydration. Thus, we have been able to construct a medium-resolution, one-dimensional electron density profile in the direction normal to the bilayer plane by performing a Fourier analysis of the (00l) diffracted intensities collected by using aligned, multilayer samples equilibrated in an atmosphere of controlled RH and temperature. Such a profile with a resolution of 5.7 Å is presented in Fig. 8. This is the only profile consistent with the swelling series data. The salient features of the profile are (i) a high electron density peak at ±19 Å arising from the electron-rich headgroup, (ii) a large, single trough at the center of the bilayer due to the terminal methyl group of the acyl chain at the sn-2 position which is of low electron density, and (iii) a region of electron

density intermediate between that of the headgroup and the terminal methyls arising from the methylene units along the length of the acyl chains. These features point to certain conditions that must be met by any model for the conformation of the lipid in the L_β phase as discussed below.

Lipid bilayer models

A complete hydration series, wherein the lipid/water ratio is varied in a known manner up to and beyond saturation, was performed on the powder samples used in this study. Thus, the relative contributions of water (d_w) and lipid (d_l) to the measured d-spacing (d) for both L_α and L_β phases has been determined. In an initial attempt to understand the arrangement of lipid molecules in the L_β and L_α phases, calculations of molecular dimensions were performed with the aid of CPK space-filling models, accepted bond lengths and angles, and measured d-spacings.

One of the 22/12 PC configurations chosen for examination is shown in Fig. 9 A. Here, the standard glycerophosphocholine configuration was used with the choline headgroup oriented approximately parallel to the bilayer surface and the glycerol backbone parallel to the all-$trans$ methylene segments of the sn-1 chain (Büldt et al., 1978). In this unstrained configuration, the molecule measures 33 ± 1.5 Å along its long axis. This is made up of (i) 7 Å for the glycerophosphocholine headgroup and includes the COO moiety of the sn-1 chain and (ii) 26 Å from the center of the CH$_2$-CO bond to the tip of the terminal methyl of the sn-1 chain. The distance between the center of the C$_\beta$-C$_\gamma$ bond of the acyl chain and the tip of the terminal methyl of the sn-2 chain is 14 Å.

With this basic configuration, a number of molecular arrangements were considered as ways in which 22/12 PC molecules assemble in the L_β and L_α phases. The model for the L_β phase is shown in Fig. 9 A. This model offers compact packing of chains and headgroups and has the terminal methyl groups on the two chains of a given lipid molecule out of register by ~12 Å. Allowing for interdigitation of chains to this extent across the bilayer midplane provides a bilayer thickness of 42 Å [(2 × 7) + (2 × 14)] with chains parallel to the bilayer normal. This bilayer thickness is consistent with the measured value (43–38 Å, Fig. 3) in the hydration range studied. The wide-angle diffraction pattern from such samples consists of a single, sharp reflection at 4.13 Å and does not show any evidence for tilting. This result suggests that the lipid molecule long axis is parallel to the bilayer normal. As can be seen from an examination of the bilayer model in Fig. 9 A the headgroup of each lipid molecule is associated with three acyl chains in the plane of the membrane. This is consistent with the membrane mensuration value of $S/\Sigma = 3$ (Table 2) indicating that the interfacial surface area per lipid molecule is approximately three times the cross-sectional area of a single acyl chain. The calculated electron density profile is in excellent agreement with the model shown in Fig. 8. The experimental data therefore suggest that the arrangement of molecules in

TABLE 2 Structure parameters of "dry" and hydrated 22/12 PC at 28°C and at 60°C derived from x-ray diffraction and density measurements.

Water concentration	d	d_l	d_w	S	Σ	S/Σ
(%w/w)	Å	Å	Å	Å²	Å²	
28°C						
0*	60.3 (4)‡	60.3	0	39.3 (0.5)§	—	—¶
0	56.9 (3)	56.9	0	41.8 (0.5)	19.9	2.10 (0.04)§
4.2	59.2 (1)	56.7	2.50	41.9 (0.5)	19.7	2.13 (0.05)
4.2	45.8 (1)	43.8	2.04	54.3 (0.9)	19.7	2.76 (0.07)
6.6	45.8 (1)	42.6	3.20	55.8 (0.9)	19.7	2.83 (0.07)
10.3	47.2 (5)	42.1	5.14	56.5 (0.9)	19.7	2.87 (0.07)
11.8	48.4 (6)	42.4	6.03	56.1 (0.9)	19.7	2.85 (0.07)
13.7	48.9 (3)	41.8	7.07	56.8 (1.0)	19.7	2.88 (0.07)
18.6	52.2 (4)	42.0	10.2	56.6 (1.0)	19.7	2.87 (0.07)
18.9	51.5 (4)	41.3	10.2	57.6 (1.0)	19.7	2.92 (0.07)
19.8	52.1 (4)	41.3	10.8	57.6 (1.0)	19.7	2.92 (0.07)
23.8	55.7 (3)	41.8	13.9	56.8 (1.0)	19.7	2.89 (0.07)
24.1	53.0 (4)	39.6	13.4	60.0 (1.1)	19.7	3.05 (0.08)
27.3	56.1 (3)	40.1	16.0	59.3 (1.1)	19.7	3.01 (0.07)
30.2	58.0 (3)	49.0	18.0	60.9 (1.1)	19.7	3.09 (0.08)
32.5	58.7 (4)	38.8	19.9	61.3 (1.1)	19.7	3.11 (0.08)
33.6	58.8 (3)	38.2	20.6	62.2 (1.2)	19.7	3.16 (0.08)
34.4	58.8 (4)	38.0	20.8			
39.1	59.2 (4)	38.3	21.0			
39.7	58.9 (3)	38.1	20.9			
43.9	59.6 (3)	38.5	21.1			
52.3	59.0 (3)	38.1	20.9			
55.0	59.0 (4)	38.2	20.9			
58.2	59.2 (4)	38.2	21.0			
66.7	59.2 (4)	38.2	21.0			
84.3	59.1 (3)	38.1	20.9			
60°C						
0*	50.4 (3)	50.4	0	50.2 (1.0)		
0	50.4 (3)	50.4	0	50.2 (1.0)		
4.2	52.3 (1)	50.1	2.2	50.4 (1.0)		
4.2	52.3 (1)	50.1	2.2	50.4 (1.0)		
6.6	52.3 (1)	48.9	3.4	51.7 (1.1)		
10.3	51.9 (4)	46.6	5.3	54.3 (1.2)		
11.8	52.0 (4)	45.8	6.2	55.2 (1.2)		
13.7	52.1 (2)	44.9	7.2	56.3 (1.2)		
18.6	53.0 (4)	43.1	9.9	58.6 (1.4)		
18.9	52.9 (3)	42.9	10.0	59.0 (1.4)		
19.8	53.9 (3)	43.2	10.7	58.5 (1.4)		
23.8	54.9 (3)	41.8	13.1	60.5 (1.4)		
24.1	53.3 (4)	40.5	12.9	62.5 (1.5)		
27.3	55.3 (3)	40.2	15.1	62.9 (1.6)		
30.2	55.5 (3)	38.7	16.8	65.3 (1.7)		
32.5	58.3 (3)	39.4	18.9	64.3 (1.6)		
33.6	57.1 (3)	37.9	19.2	66.7 (1.8)		
34.4	66.3 (3)	43.5	22.8	58.2 (1.3)		
39.1	65.7 (3)	40.0	25.7	63.2 (1.6)		
39.7	67.9 (2)	40.9	27.0	61.8 (1.5)		
43.9	68.3 (2)	38.9	29.4			
52.3	71.8 (2)	40.9	30.9			
55.0	71.6 (2)	40.8	30.8			
58.2	70.3 (2)	40.1	30.2			
66.7	71.6 (2)	40.8	30.8			
84.3	70.7 (2)	40.3	30.4			

*This sample was not preheated. The rest of the samples were preheated as described under Experimental Procedures.

‡Numbers in parentheses in this column correspond to the number of lamellar reflections observed.

§Numbers in parentheses in this column correspond to relative error. For example, in the case of S (Å²), the relative error is

$S \times \sqrt{(\Delta v_1/v_1)^2 + (\Delta d_1/d_1)^2}$, where Δ refers to the estimated uncertainty in the measured quantity.

¶This non-preheated sample is in the L_c phase. Values of S are calculated only for lemellar gel phases (Eq. 8).

the lipid bilayer is of the so-called mixed interdigitated type (L_β^m (Hui et al., 1984; McIntosh et al., 1984)) as shown in the figure.

In the dry condition, 22/12 PC forms a single lamellar crystalline (L_c) phase in the absence of prior heat treatment. Without water $d_w = 0$, the lamellar d-spacing corresponds to

d_1 and measures 60.3 Å. The d-spacing suggests that the chain packing is of the partially interdigitated type. CPK models of such a phase give a headgroup contribution to the d-spacing of 10 Å measured from the tip of the terminal methyls of choline and including the COO moiety of the sn-1 chain.
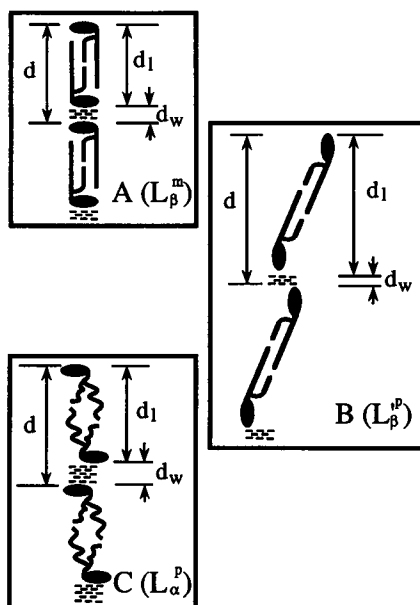
FIGURE 9 Diagrammatic representation of the various lamellar configurations adopted by 22/12 PC as discussed in the text. $(A)\,L_\beta^m$; $(B)\,L_{\beta'}^p$; and $(C)\,L_\alpha^p$. The solid figures represent the lipid molecules with straight, and wavy lines corresponding to the ordered and disordered acyl chains, respectively. The horizontal dashes represent water molecules. The lamellar repeat (d), water layer thickness (d_w), and lipid bilayer thickness (d_l) dimensions are indicated.

When dry 22/12 PC is subjected to a preheating treatment the lipid forms a single, possibly metastable, lamellar gel phase. The lamellar repeat is 56.9 Å at 28°C, and the diffraction pattern shows a sharp reflection at 4.21 Å with a wide-angle shoulder at 4.19 Å reminiscent of the $L_{\beta'}$ phase of hydrated symmetric PC homologs. In the case of the $L_{\beta'}$ phase the acyl chains are tilted with respect to the bilayer normal. A molecular arrangement consistent with these observations is presented in Fig. 9 B. It shows 22/12 PC in the lamellar, so-called partially interdigitated gel phase $(L_{\beta'}^p)$ wherein the chains interdigitate. In contrast to the L_β^m phase, chain interdigitation in the $L_{\beta'}^p$ is incomplete. This means that the acyl chains from lipid in one leaflet of the bilayer do not extend all the way across the bilayer but rather meet one another in the bilayer interior with the terminal methyls at the sn-1 and sn-2 positions from adjacent leaflets touching. The lipid bilayers so formed have two acyl chains/headgroup on average consistent with an S/Σ value of 2.10 recorded in Table 2.

Interestingly, we find coexistence of the partially and mixed interdigitated phases at hydration levels intermediate between the dry and more fully hydrated condition. The preheated dry lipid adopts the former, while hydrated lipid assumes the latter configuration. Only two measurements were made in this region of intermediate hydration. In both cases, a limited number of low-angle reflections were observed making unambiguous phase identification impossible. The following rationale was used in making the above tentative phase assignments. In the case of the sample at 6.6% (w/w)

water a single, low-angle reflection at 45.8 Å was observed at 28°C. If we assume that this corresponds to the (001) reflection of a lamellar phase and perform membrane mensuration calculations as above we find the following repeat parameters: d = 45.8 Å, d_1 = 42.6 Å, and d_w = 3.2 Å. Referring to Fig. 3, the repeat parameters of the L_β^m phase change monotonically with water concentration in the range 10.3 to 34% (w/w). Extrapolating these plots back to 6.6% (w/w) water gives the following repeat parameter values: d = 45.2 Å, d_1 = 42.0 Å, and d_w = 3.2 Å in close agreement with the values noted above. This lends support to our tentative identification of the phase observed at 28°C and 6.6% (w/w) water as being of the L_β^m type. Consistent with this designation is the observation made during the swelling series experiments that the intensities of the higher order reflections from the L_β^m phase are likely to be weak at this low hydration level (see Fig. 7).

The sample at 4.2% (w/w) water and 28°C has been proposed to consist of co-existing L_β^m and $L_{\beta'}^p$ phases. However, only two reflections are seen in the low-angle region of the diffraction pattern at 45.8 and 59.2 Å. If we assume that these correspond to the (001) reflections of the L_β^m and $L_{\beta'}^p$ phases, respectively, membrane mensuration calculations give S/Σ values of 3 and 2, respectively, as expected. Thus, the reflection at 59.2 Å can be compared with the lamellar repeat d-spacing of the $L_{\beta'}^p$ phase in the dry lipid at 56.9 Å. In turn, the reflection at 45.8 Å can be compared with the lamellar repeat value 43.2 Å obtained by extrapolating back to 4.2% (w/w) water in the d-spacing hydration plot in Fig. 3. The difference between these last two values most likely reflects the presence in the corresponding temperature-composition phase diagram of a phase coexistence region where, at a fixed temperature, it is the relative amounts of the two coexisting phases that change with overall composition and not the actual water content, and thus, d-spacing of the phase.

In the excess water region beyond the hydration limit, passage through the order/disorder transition is accompanied by a 20% increase in lamellar repeat spacing from 59 to 71 Å when data are compared at 28 and 60°C. The membrane mensuration data (Table 2) show how the various compartments within the unit cell change as a result of the heating transition. Interestingly, the size of the water layer between lamellae increases from 21 to 30 Å, while the bilayer thickness undergoes an unexpected increase also from 38 to 41 Å. It is unexpected because for a simple chain order/disorder transition the introduction of trans/gauche rotational isomerization in the chain at high temperatures has the effect of lowering the effective length of the chains (Cevc and Marsh, 1987). Undoubtedly, this effect is occurring during the transition in question. However, it must also be accompanied by at least one other structural rearrangement to cause the overall bilayer thickness to increase as it does. We propose, therefore, that in addition to chain "melting" the lipid molecules, which start out at low temperature in the L_β^m phase, undergo a structural rearrangement so that the molecules end up in the L_α phase with an orientation akin to that found in the partially

interdigitated phase. In the L_β^m phase, space-filling CPK models give a bilayer thickness of 42 Å. A reduction in bilayer thickness of ~5 Å is expected for methylene segment melting only. This calculation assumes a contribution of 1.00 and 1.26 ± 0.01 Å per methylene group above and below the transition temperature, respectively (Tardieu et al., 1973; Hauser and Shipley, 1983). However, in the $L_{\beta'}^p$ phase space-filling models give a bilayer thickness of 60 Å and a reduction by ~8 to 52 Å upon methylene segment melting only. Since the L_β^p-to-L_α transition is accompanied by an increase of interfactial area per lipid molecules, it is possible that in the L_α phase the headgroup is oriented more or less parallel to the bilayer plane which accounts for a further reduction in d_1 by ~6 to 46 Å. The later is consistent with the measured lipid bilayer (38–41 Å) in the hydration region studied (Table 2 and Fig. 3). We conclude therefore that the lipid chains are partially interdigitated in the L_α phase (L_α^p, Fig. 9 C).

Temperature-composition phase diagram

A summary of the mesophase behavior of the 22/12 PC-water system in temperature-composition (T-C) space is presented in the form of a T-C phase diagram in Fig. 10. The diagram has been constructed most thoroughly in the 25–65°C tem-
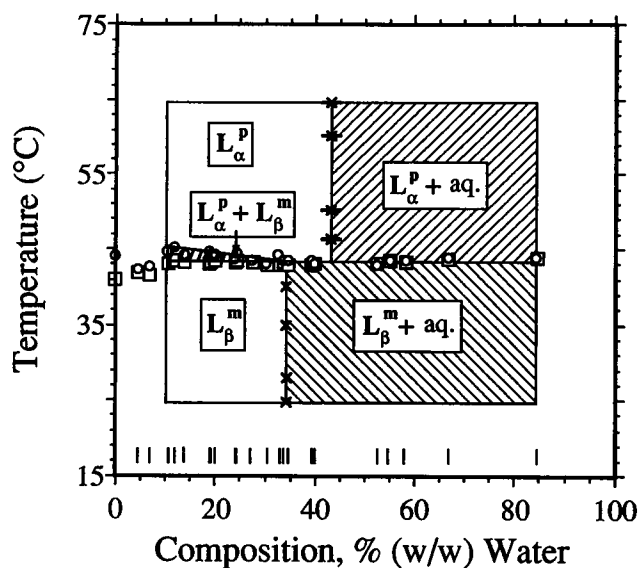

FIGURE 10　Temperature-composition phase diagram of 22/12 PC in water obtained by using time-resolved x-ray diffraction isoplethally in the heating direction. The onset (□) and completion (○) temperatures of the chain order/disorder transition correspond to the lowest and highest temperatures of phase coexistence observed in the streak film data of the type shown in Fig. 2 A. The hydration limit is marked with an x and was determined at several temperatures from swelling data of the type shown in Fig. 3. The area surrounded by a rectangle indicates the region of the phase diagram that has been investigated continuously in temperature from 25 to 65°C and at the composition values indicated by the tick marks located above the abscissa. Single and two phase regions are identified in the rectangle by the clear and cross-hatched areas, respectively. A degree of uncertainty is associated with determining the position of the hydration limit boundary for the L_α^p phase. This is so indicated by horizontal bars.

perature range and in the 10.3–84.3% (w/w) water concentration range. This region of the phase diagram is identified by a closed rectangle in the figure. A limited amount of data has been obtained below 10% (w/w) water that will be treated separately. The data enclosed by the rectangle was collected by using x-ray diffraction for phase identification and structure characterization continuously in temperature in the heating direction isoplethally. The position of the boundaries separating the L_β^m and L_α^p phases was easily determined along each isopleth as the temperature or temperature range where the phase transition occurred. Such transition temperatures are easily determined from the streak film data as shown in Fig. 2. The boundaries of limiting hydration beyond which an excess water phase appears were identified based on hydration plots of the type shown in Fig. 3. The boundary marks the hydration level where the lamellar repeat stabilizes. This is known with considerable accuracy in the case of the L_β^m phase. However, because of a pronounced curvature in the water concentration dependence of the various lamellar repeat parameters of the L_α^p phase close to the hydration limit (Fig. 3 B) there is somewhat more uncertainty in the position of the corresponding boundary for the L_α^p phase. This is so indicated in the phase diagram by horizontal bars in the figure.

For purposes of discussion the T-C phase diagram can be viewed as being composed of four quadrants. The two lower quadrants correspond to the low temperature L_β^m phase where the quadrant on the left hand side represents the pure L_β^m phase, while that on the right corresponds to the region of T-C space where L_β^m and an aqueous phase coexist. The two upper quadrants correspond to the high temperature L_α^p phase. To the left is the pure L_α^p phase and to the right is the L_α^p phase coexisting with excess aqueous medium.

There are several novel features associated with this phase diagram. To begin with, the boundaries separating the water-stressed from the fully hydrated phases are essentially independent of temperature to within the error limits of these measurements. Second, in the water-stressed region between ~0 and 45% (w/w) water the chain order/disorder transition temperature shows very little dependence on water content. What we find in this region is that the onset temperature remains essentially unchanged at 43°C, while the completion temperature rises from 43°C at 35% (w/w) water to 44°C at 0% (w/w) water. This is in distinct contrast to the behavior of the symmetric PCs which shows a pronounced increase in the chain order/disorder transition temperature with dehydration (Gottlieb and Eanes, 1974; Ulmius et al., 1977; Grabielle-Madelmont and Perron, 1983). Third, the L_β^m-to-L_α^p transition takes place without the appearance of an intermediate phase such as the ripple or $P_{\beta'}$ phase as is observed with the symmetric PCs (Janiak et al., 1979; Kodama et al., 1982; Grabielle-Madelmont and Perron, 1983). It is true that the low temperature phase is different for the symmetric and asymmetric PCs. In the former case, the low temperature phase is of the $L_{\beta'}$ type with tilted chains and minimal interdigitation of chain termini at the bilayer midplane. With the L_β^m phase, however, interdigitation is complete. It

may be, therefore, that a prerequisite for the heat-induced formation of the $P_{\beta'}$ phase is a mesophase structure of the $L_{\beta'}$ type. It will be instructive to establish the limits of chain inequivalence tolerated by the PCs beyond which the $P_{\beta'}$ phase is no longer stable as an intermediate between the lamellar gel and lamellar liquid crystal phases.

While the absence of the $P_{\beta'}$ phase in the T-C phase diagram of 22/12 PC is intriguing, of equal interest is its ability to form the interdigitated L_{β}^{m} phase. To date, there are only two other PC species that have been reported to exhibit this behavior when hydrated (and without additives), namely, 1-stearoyl-2-caproyl-sn-glycero-3-phosphocholine (18/10 PC) and 1-octanoyl-2-stearoyl-sn-glycero-3-phosphocholine (8/18 PC), both highly asymmetric PCs (McIntosh et al., 1984; Shah et al., 1990). A feature common to all three lipids is a $\Delta C/CL$ value of 0.5–0.6.

To within the limits of our measurements, the phase diagram appears to be consistent with the Gibb's phase rule in that single phase regions are separated by regions of two phase coexistence. Furthermore, the two phase regions are separated by one phase or three phase regions, and the latter only by two phase regions.

Mesophase thermal expansion

Much of the data in this study was collected using streak film where the influence of temperature on structure parameter dimensions is immediately apparent. Accordingly, the thermal expansion coefficient defined as

$$\alpha = (1/\eta)(\Delta\eta/\Delta T) \qquad (9)$$

where η is the parameter under consideration and T is temperature, has been calculated for both the long- and short-range periodic structures within the lamellar phase as a function of hydration level. The quantity α can be viewed as the responsivity of the given lattice dimension to temperature normalized to a particular reference lattice size. In the case of the L_{β}^{m} phase, α values can be calculated which refer to the thermal responsivity of the lamellar repeat (d), the lipid bilayer thickness (d_l), the water layer thickness (d_w), the acyl chain repeat spacing (d_c), and the lipid-water interfacial area (S). These data are presented graphically in Fig. 11. Since the scattering from the chains in the L_{α}^{p} phase is weak and diffuse the temperature dependence of chain disorder was not examined and only the α value for the lamellar repeat spacing is reported in this study (Fig. 11 A).

The α value for the chain-packing lattice parameter in the L_{β}^{m} phase is small, positive and quite insensitive to hydration (Fig. 11 F). This indicates that the chain-packing lattice size increases only slightly with temperature and in a manner which is independent of lipid hydration in the region studied. In contrast, the lamellar repeat parameter in the L_{β}^{m} phase has a negative α-value below the hydration limit beyond which it becomes totally insensitive to temperature and hydration level in the range studied (Fig. 11 B). Qualitatively, the same behavior is found for d_l and d_w in the L_{β}^{m} phase (Fig. 11, C and D) in the water-stressed region. At full hydration and
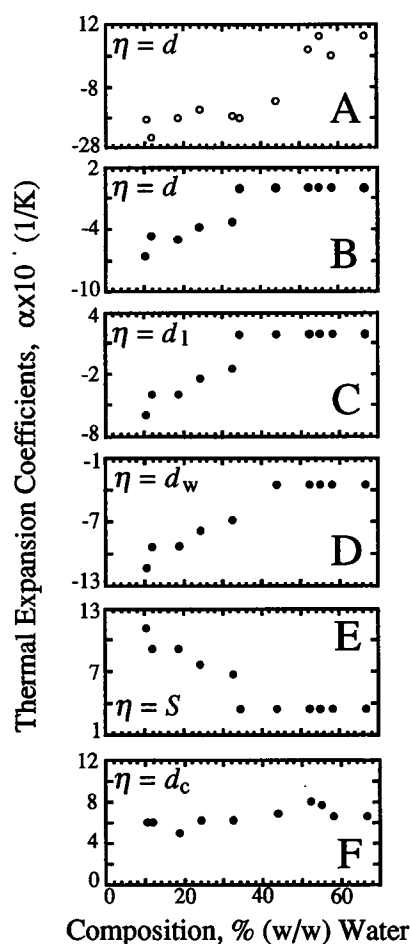

FIGURE 11　Hydration dependence of the thermal expansion coefficient (α) of the L_{β}^{m} and L_{α}^{p} phases formed by 22/12 PC. (A) α values (Eq. 9) for the lamellar repeat (d) in the L_{α}^{p} phase. α values for the lamellar repeat (d), bilayer (d_l), and water layer thickness (d_w), lipid interfacial area (S) and for the chain-packing parameter (d_c) in the L_{β}^{m} phase are shown in B, C, D, E, and F, respectively. The corresponding temperature values in Eq. 9 are 28 and 60°C for the L_{β}^{m} phase and 46 and 60°C for the L_{α}^{p} phase with the higher temperature used as the reference state in both phases.

beyond, d_l and d_w respond oppositely to temperature such that the net effect is a thermally insensitive lamellar repeat (d) in this same region. The α value for the L_{β}^{m} lipid interfacial area is positive below the hydration limit (Fig. 11 E). The α value drops but does not change sign when full hydration is reached.

The situation is somewhat different in the case of the lamellar repeat parameter of the L_{α}^{p} phase. It exhibits a large negative α value below and a small positive α value above the hydration limit.

Comparison with other systems and other studies

The calorimetric properties of 22/12 PC have been studied under conditions of full hydration. For example, upon heating at a rate of 10–15°C/h in the range 10 to 60°C, Lin et al. (1990) found a single, sharp endothermic transition at 43.4°C

(ΔH = 13.5 kcal/mol). This transition was reproduced in a second heating scan. Our data show this to be the L_β^m-to-L_α^p transition. On cooling at a rate of 5–15°C/h, two exothermic transitions were found, one at 42.7°C and the other at 38.6°C (Fig. 2 C). The sum of the two exothermic transition enthalpies was 13.0 kcal/mol. Upon repeated heating-cooling cycles the area under the low temperature exothermic transition at 38.6°C increased at the expense of that associated with the cooling transition at 42.7°C. While the cooling behavior of the fully hydrated 22/12 PC system was not examined in detail in the present study, it is interesting to note the correspondence between the diffraction and the calorimetric data as shown in Fig. 2, B and C.

The calorimetric behavior of 22/12 PC described above is similar to that of 18/10 PC as studied by Boggs and Mason (1986). Interestingly, the $\Delta C/CL$ of these two lipids is very similar (0.559 vs. 0.548 for 22/12 PC). Freshly prepared and fully hydrated 18/10 PC shows a single heating endotherm and a single cooling exotherm centered some 4°C below the heating transition. Both transitions have the same associated enthalpy change. When the samples are subjected to prolonged storage at −20°C the temperature of the cooling transition increases and develops into two poorly resolved exothermic peaks. After repeated cycling through the main transition, the size of the lower temperature exothermic cooling peak increases at the expense of that at the higher temperature. Thermal history had no effect on the heating endotherm.

Calorimetric behavior which includes a single heating endotherm and multiple cooling exotherms is not confined to the asymmetric PCs. For example, fully hydrated 1-stearoyl-2-caproyl-sn-glycero-3-phosphoethanolamine (18/10 PE) exhibits such behavior with a single asymmetric endothermic transition at 21.1°C and two partially overlapping cooling exotherms, one at 20.1°C and the other at 17.9°C (Mason and Stephenson, 1990). The cooling transitions were found to be sensitive to scan rate, while the heating transition was not. The high temperature cooling exotherm was attributed to an L_α-to-L_β^p transition and the lower temperature exotherm to an L_β^p-to-L_β^m transition. Other lipid systems that exhibit a

single heating transition and multiple cooling transitions of the type seen with 22/12 PC include 1-palmitoyl-2-oleoyl-sn-glycero-3-phosphoethanolamine and 1,2-dielaidoyl-sn-glycero-3-phosphoethanolamine (Epand and Epand, 1988) and 1,2-dipalmitoyl-sn-glycero-3-phosphoethanolamine (Yao et al., 1992). The origin of these curious cooling transitions is still in question and is worthy of further investigation.

The mixed interdigitated lamellar gel phase has been reported in the literature previously. Thus, for example, Hui et al. (1984) proposed the existence of the L_β^m phase in fully hydrated 18/10 PC and 18/12 PC based on x-ray diffraction and electron microscopy measurements. In like manner, McIntosh et al. (1984) demonstrated the existence of the L_β^m phase above 10% (w/w) water in 18/10 PC by using x-ray diffraction. In this case, the lamellar repeat spacing was found to be 12 Å smaller than that expected for the more common $L_{\beta'}$ phase suggesting interdigitation of the mixed type. Furthermore, a sharp, symmetric wide-angle reflection at 4.11 Å indicated that the chains were not tilted. A measured S/Σ value of 3 lent additional support for the L_β^m model. Recently, Shah et al. (1990) have reported finding the L_β^m phase in a fully hydrated 8/18 PC system at low temperatures. Again, a single, symmetric wide-angle reflection at 4.1 Å was found suggesting untilted chains as observed by McIntosh et al. (1984) for 18/10 PC and in the present study for 22/12 PC. Interestingly, in the case of 8/18 PC an increase in bilayer thickness of 6 Å was observed upon heating through the chain order/disorder transition. This result is in qualitative agreement with those obtained in the current study. As noted above, the L_β^m phase has been proposed to exist in the asymmetric PEs also (Mason and Stephenson, 1990).

A lamellar crystalline phase reminiscent of the partially interdigitated lamellar gel phase has been reported previously by Tardieu et al. (1973) for 18/10 PC under conditions of low hydration. It may be a characteristic of this phase that it is expressed at extremely low hydration levels as was found in the case of 22/12 PC in the current investigation.

TABLE 3 Miscibility of lipid-lipid binary systems

Group	Binary system, ($\Delta C/CL$)	Miscibility* Gel phase	Miscibility* Fluid phase	References
I	18/18 PC (0.088)–18/16 PC (0.206)	c.m.	c.m.	Mason (1988)
	18/18 PC (0.088)–18/14 PC (0.324)	c.m.	c.m.	Mason (1988)
	16/16 PC (0.088)–12/20 PC (0.371)	c.m.	c.m.	Bultmann et al. (1991a)
II	20/12 PC (0.500)–10/22 PC (0.538)	c.m.	c.m.	Bultmann et al. (1991a)
	22/12 PC (0.548)–10/22 PC (0.538)	c.m.	c.m.	Xu et al. (1987)
III	18/18 PC (0.088)–18/12 PC (0.441)	p.m.	c.m.	Mason (1988)
	17/17 PC (0.094)–22/12 PC (0.548)	p.m.	c.m.	Bultmann et al. (1991b)
	16/16 PC (0.088)–10/22 PC (0.538)	p.m.	c.m.	Bultmann et al. (1991a)
	14/14 PC (0.115)–18/10 PC (0.559)	p.m.	c.m.	Lin and Huang (1988)
	18/18 PC (0.088)–18/10 PC (0.559)	p.m.	p.m.	Mason (1988)

*c.m. and p.m. refer to completely miscible and partially miscible, respectively.

In addition to studies on the thermotropic and lyotropic mesomorphism of the asymmetric PCs, a limited number of measurements have been performed on the miscibility of these lipids with other symmetric and asymmetric PCs. An interesting trend emerges from an examination of the miscibility properties of these systems as summarized in Table 3. In this table, the binary lipid systems have been arranged into three groups. Group I includes binary mixtures of symmetric and asymmetric ($\Delta C/CL = 0.21$–0.37) PCs. In this group, complete miscibility is seen in both the gel and liquid crystalline phases. Again, complete miscibility is observed in the low and high temperature phases with Group II binary mixtures where both lipids are asymmetric to nearly the same degree ($\Delta C/CL = 0.50$–0.54). Group III includes mixtures of symmetric and highly asymmetric ($\Delta C/CL = 0.44$–0.56) PCs. In this case, only partial miscibility is seen in the gel phase. Miscibility in the L_α phase is complete in all Group III systems with the exception of 18/18 PC in combination with 18/10 PC where partial miscibility in the L_α phase prevails. While the database is limited, a pattern of behavior is apparent in this series. Thus, complete miscibility obtains when the lipids in the binary mixture are equally symmetric or asymmetric or in the case of symmetric/asymmetric mixtures when the degree of asymmetry is not extreme. Otherwise, incomplete miscibility is observed consistently in the low temperature phase. This behavior can extend into the L_α phase under certain limiting circumstances. Broadening the scope of this database in all categories will facilitate enormously the establishment of the principles underlying lipid/lipid miscibility and our understanding of lipid miscibility related phenomena in biological membranes.

SUMMARY

X-ray diffraction and specific volume measurements coupled with mesophase mensuration on oriented and powder samples of a highly asymmetric phospholipid, 22/12 PC, have been performed with temperature and lipid hydration as variables. The corresponding T-C phase diagram shows some significant departures from the behavior of the symmetric PCs, the most notable of which include the absence of a $P_{\beta'}$ phase between the lamellar gel and liquid crystal phases, a weak dependence of chain order/disorder transition temperature on hydration, and a pronounced tendency for chain interdigitation in the assorted lamellar phases found. All of the phases encountered in this study have undergone careful structure characterization, and in each case the dependence of the various lattice parameters on temperature and on hydration has been measured. Furthermore, thermomechanical properties of the lipid and aqueous compartments within these phases and their dependence on hydration have been established. Our next most immediate objective is to extend this study to related asymmetric PCs and other phospholipid classes and to examine in greater detail the miscibility properties of the symmetric and asymmetric phospholipids. The long term goal is to establish the relationship between lipid molecular structure, sample composition, mesophase behavior, and miscibility in an attempt to decipher the assorted interactions taking place in cellular and reconstituted membranes.

REFERENCES

Boggs, J. M., and J. T. Mason. 1986. Calorimetric and fatty acid spin label study of subgel and interdigitated gel phases formed by asymmetric phosphatidylcholines. *Biochim. Biophys. Acta.* 863:231–242.

Büldt, G., H. U. Gally, A. Seelig, J. Seelig, and G. Zaccai. 1978. Neutron diffraction studies on selectively deuterated phospholipid bilayers. *Nature (Lond.).* 271:182–184.

Bultmann, T., H. Lin, Z. Wang, and C. Huang. 1991a. Thermotropic and mixing behavior of mixed-chain phosphatidylcholines with molecular weights identical with that of L-α-dipalmitoylphosphatidylcholine. *Biochemistry.* 30:7194–7202.

Bultmann, T., W. L. C. Vaz, E. C. C. Melo, R. B. Sisk, and T. E. Thompson. 1991b. Fluid-phase connectivity and translational diffusion in a eutectic, two-component, two-phase phosphatidylcholine bilayer. *Biochemistry.* 30:5573–5579.

Caffrey, M. 1984. X-radiation damage of hydrated lecithin membranes detected by real-time x-ray diffraction using wiggler-enhanced synchrotron radiation as the ionizing radiation source. *Nucl. Instr. and Meth. in Phys. Res.* 222:329–338.

Caffrey, M. 1985. Kinetics and mechanism of the lamellar gel/lamellar liquid-crystal and lamellar/inverted hexagonal phase transition in phosphatidylethanolamine: a real-time x-ray diffraction study using synchrotron radiation. *Biochemistry.* 24:4826–4844.

Caffrey, M. 1987. Kinetics and mechanism of transitions involving the lamellar, cubic, inverted hexagonal, and fluid isotropic phases of hydrated monoacylglycerides monitored by time-resolved x-ray diffraction. *Biochemistry.* 26:6349–6363.

Caffrey, M., J. Hogan, and A. S. Rudolph. 1991a. Diacetylenic lipid microstructures: structural characterization by x-ray diffraction and comparison with the saturated phosphatidylcholine analogue. *Biochemistry.* 30:2134–2146.

Caffrey, M., D. Moynihan, and J. Hogan. 1991b. A database of lipid phase transition temperatures and enthalpy changes. *J. Chem. Inf. Comput. Sci.* 31:275–284.

Cevc, G., and D. Marsh. 1987. Phospholipid Bilayers, Physical Principles and Models. Wiley-Interscience, New York. 19–24.

Cheng, A.-C., J. L. Hogan, and M. Caffrey. 1993. X-ray destroy the lamellar structure of model membrane. *J. Mol. Biol.* 229:291–294.

Chung, H., and M. Caffrey. 1992. Direct correlation of structure changes and thermal events in hydrated lipid established by simultaneous calorimetry and time-resolved x-ray diffraction. *Biophys. J.* 63:438–447.

Epand, R. M., and R. F. Epand. 1988. Kinetic effects in the differential scanning calorimetry cooling scans of phosphatidylethanolamines. *Chem. Phys. Lipids.* 49:101–104.

Gottlieb, M. H., and E. D. Eanes. 1974. Coexistence of rigid crystalline and liquid crystalline phases in lecithin-water mixtures. *Biophys. J.* 14:335–342.

Grabielle-Madelmont, C., and R. Perron. 1983. Calorimetric studies on phospholipid-water systems. I. DL-Dipalmitoylphosphatidylcholine (DPPC)-water system. *J. Colloid Interface Sci.* 95:471–482.

Hauser, H., and G. G. Shipley. 1983. Interactions of monovalent cations with phosphatidylserine bilayer membranes. *Biochemistry.* 22:2171–2178.

Huang, C. 1991. Empirical estimation of the gel to liquid-crystalline phase transition temperatures for fully hydrated saturated phosphatidylcholines. *Biochemistry.* 30:26–30.

Hui, S. W., J. T. Mason, and C. Huang. 1984. Acyl chain interdigitation in saturated mixed-chain phosphatidylcholine bilayer dispersions. *Biochemistry.* 23:5570–5577.

Janiak, M. J., D. M. Small, and G. G. Shipley. 1979. Temperature and compositional dependence of the structure of hydrated dimyristoyl lecithin. *J. Biol. Chem.* 254:6068–6078.

Klose, G., B. König, H. W. Meyer, G. Schulze, and G. Degovics. 1988. Small-angle x-ray scattering and electron microscopy of crude dispersions of swelling lipids and the influence of the morphology on the repeat distance. *Chem. Phys. Lipids.* 47:225–234.

Klose, G., B. König, and F. Paltauf. 1992. Sorption isotherms and swelling of POPC in H_2O and ^2H_2O. *Chem. Phys. Lipids.* 61:265–270.

Kodama, M., M. Kuwabara, and S. Seki. 1982. Successive phase-transition phenomena and phase diagram of the phosphatidylcholine-water system as revealed by differential scanning calorimetry. *Biochim. Biophys. Acta.* 689:567–570.

Lin, H., and C. Huang. 1988. Eutectic phase behavior of 1-stearoyl-2-caprylphosphatidylcholine and dimyristoylphosphatidylcholine mixtures. *Biochim. Biophys. Acta.* 946:178–184.

Lin, H., Z. Wang, and C. Huang. 1990. Differential scanning calorimetry study of mixed-chain phosphatidylcholines with a common molecular weight identical with diheptadecanoylphosphatidylcholine. *Biochemistry.* 29:7063–7072.

Lin, H., Z. Wang, and C. Huang. 1991. The influence of acyl chain-length asymmetry on the phase transition parameters of phosphatidylcholine dispersions. *Biochim. Biophys. Acta.* 1067:17–28.

Luzzati, V. 1968. X-ray diffraction studies of lipid-water systems. *In* Biological Membranes, Physical Fact and Function. Vol. 1. D. Chapman, editor. Academic Press, New York. 71–123.

Mason, J. T. 1988. Mixing behavior of symmetric chain length and mixed chain length phosphatidylcholines in two-component multilamellar bilayers: evidence for gel and liquid-crystalline phase immiscibility. *Biochemistry.* 27:4421–4429.

Mason, J. T., C. Huang, and R. L. Biltonen. 1981. Calorimetric investigations of saturated mixed-chain phosphatidylcholine bilayer dispersions. *Biochemistry.* 20:6086–6092.

Mason, J. T., and F. A. Stephenson. 1990. Thermotropic properties of saturated mixed acyl phosphatidylethanolamines. *Biochemistry.* 29:590–598.

Mattai, J., P. K. Sripada, and G. G. Shipley. 1987. Mixed-chain phosphatidylcholine bilayers: structure and properties. *Biochemistry.* 26:3287–3297.

McIntosh, T. J., S. A. Simon, J. C. Ellington, Jr., and N. A. Porter. 1984. New structural model for mixed-chain phosphatidylcholine bilayers. *Biochemistry.* 23:4038–4044.

Mencke, A. P., and M. Caffrey. 1991. Kinetics and mechanism of the pressure-induced lamellar order/disorder transition in phosphatidylethanolamine: a time resolved x-ray diffraction study. *Biochemistry.* 30:2453–2463.

O'Brien, F. E. M. 1948. The control of humidity by saturated salt solutions. *J. Sci. Instrum.* 25:73–76.

Shah, J., P. K. Sripada, and G. G. Shipley. 1990. Structure and properties of mixed-chain phosphatidylcholine bilayers. *Biochemistry.* 29:4254–4262.

Small, D. M. 1967. Phase equilibria and structure of dry and hydrated egg lecithin. *J. Lipid Res.* 8:551–557.

Small, D. M. 1986. Handbook of Lipid Research, The Physical Chemistry of Lipids. Plenum Publishing Corp., New York. 1–19.

Tardieu, A., V. Luzzati, and F. C. Reman. 1973. Structure and polymorphism of the hydrocarbon chains of lipids: a study of lecithin-water phases. *J. Mol. Biol.* 75:711–733.

Ulmius, J., H. Wennerström, G. Lindblom, and G. Arvidson. 1977. Deuteron nuclear magnetic resonance studies of phase equilibria in a lecithin-water system. *Biochemistry.* 16:5742–5745.

Wang, Z., H. Lin, and C. Huang. 1990. Differential scanning calorimetric study of a homologous series of fully hydrated saturated mixed-chain C(X):C(X+6) phosphatidylcholines. *Biochemistry.* 29:7072–7076.

Xu, H., F. A. Stephenson, and C. Huang. 1987. Binary mixtures of asymmetric phosphatidylcholines with one acyl chain twice as long as the other. *Biochemistry.* 26:5448–5453.

Yao, H., I. Hatta, R. Koynova, and B. Tenchov. 1992. Time-resolved x-ray diffraction and calorimetric studies at low scan rates. *Biophys. J.* 61:683–693.

Zaccai, G., G. Büldt, A. Seelig, and J. Seelig. 1979. Neutron diffraction studies on phosphatidylcholine model membranes. *J. Mol. Biol.* 134:693–706.